A novel Power-Increment Based GMPPT Algorithm for PV Arrays Under Partial Shading Conditions

Xingshuo Li[a,b], Huiqing Wen[a,*], Guanying Chu[a,b], Yihua Hu[b], Lin Jiang[b]

[a] *Department of Electrical and Electronic Engineering, Xian Jiaotong-Liverpool University, Suzhou 215123, China*
[b] *Department of Electrical Engineering and Electronics, University of Liverpool, Liverpool L69 3GJ, United Kingdom*

Abstract

Due to dust, structural interfering from surrounding buildings or trees, partial shading conditions (PSCs) are frequently occurred in photovoltaic (PV) arrays, which affects the generated power and system reliability significantly. Under PSCs, PV arrays exhibit multiple local maximum power points (LMPPs), which make the conventional maximum power point tracking (MPPT) algorithms difficult to quickly allocate the optimal operating point with the maximum output power. In order to solve this issue, a novel power-increment based global MPPT (GMPPT) algorithm is proposed by combining the voltage line, the load line, and the power line altogether in determining the tracking direction and the step size. The proposed algorithm retains the advantages of the conventional power incremental based GMPPT technique. Moreover, it can realize a successful convergence to the GMPP under any pattern of PSC, which is difficult to accomplish for some GMPPT algorithms. It

*Corresponding author
Email addresses: X.Li31@liverpool.ac.uk, Xingshuo.Li@xjtlu.edu.cn (Xingshuo Li), Huiqing.Wen@xjtlu.edu.cn (Huiqing Wen)

simplifies the control implementation since it is not necessary to know exactly the internal connection of the PV array for the practical implementation of the algorithm. Furthermore, the proposed algorithm shows improved tracking speed and higher accuracy than other GMPPT techniques. It directly regulates the duty-cycle of the power interface rather than the output power command. Thus, the circuit design becomes easier. Finally, various partial shading scenarios are evaluated experimentally in order to validate the effectiveness of the proposed algorithm.
Keywords: Partial shading condition (PSC), tracking speed, GMPPT, power converter.

Partial shading is defined that one or several PV modules in a complicated PV array are shading due to dust, structural interfering from the surrounding buildings, trees or poles. The shaded modules can not produce power. Instead, they act as the load and produce heat. The worse scenario is that the string current will fall to zero and lose all the power due to one or several shaded PV modules in the string. It was reported that high up to 41% of the install PV arrays in Germany had been experienced by the partial shading conditions (Drif et al., 2008).

Under the partial shading conditions (PSC), the characteristics of PV arrays show multiple local maximum power points (MPPs), as shown in Fig. 1(b). As illustrated in Fig. 1(a), there is only one MPP on the classic P-V curve for PV arrays operate with uniform illumination. Thus, many conventional maximum power point tracking (MPPT) methods, such as Perturb and Observe (P&O) (Femia et al., 2005; Elgendy et al., 2015), Incremental Conductance (INC) method (Elgendy et al., 2013; Soon and Mekhilef, 2014),

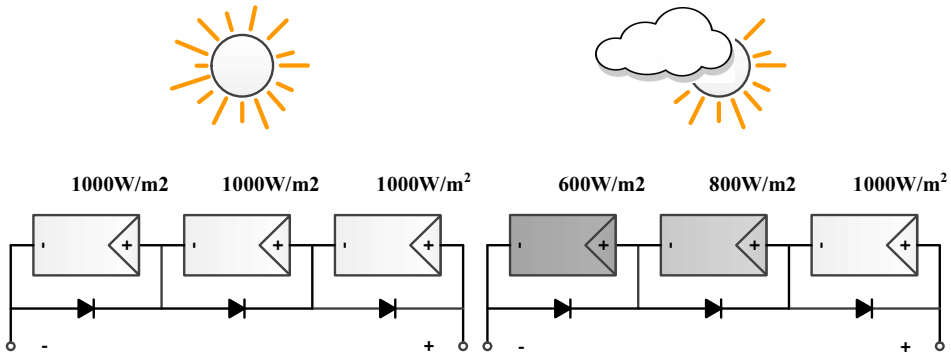

Fig. 1: A PV string under (a)uniform insolation condition; (b)partial shadowing condition.

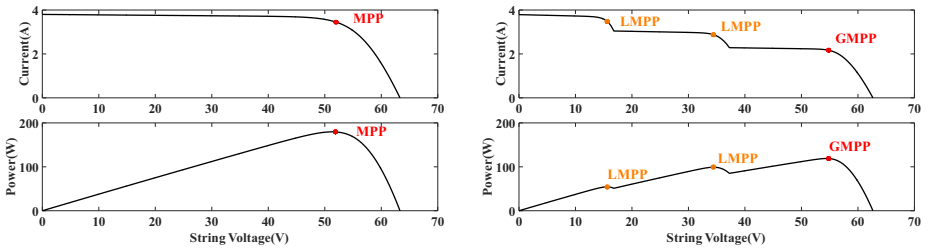

Fig. 2: I-V and P-V curves for the PV string under (a)uniform condition; (b)partial shadowing condition.

and Beta method (Li et al., 2016a,b) are unable to distinguish the global maximum power point (GMPP) from the local maximum power points (LMPP), as shown in Fig. 2(b). Consequently, both the generated power and the system reliability are significantly affected. As stated by the real data, the measured power loss due to the wrong tracking of operating point at LMPPs instead of GMPP is high up to 70% (Petrone et al., 2008).

To address this issue, many hardware-based methods have been discussed including the bypass diodes method, reconfiguration of PV modules, dis-

tributed MPPT (DMPPT), and differential power processing (DPP). Bypass diodes are widely used to relieve the power loss due to the partial shading. However, the reduction of output power is significant since the bypassed PV cell substring is unable to work properly and the string current is affected by the shaded PV cells (Bidram et al., 2012). Non-uniform aged PV modules reconfiguration has been proposed for large-scale PV array using an optimization model (Hu et al., 2017). However, all possible configurations within the PV array must be known before the optimization. Furthermore, a matrix of power switches or relays are usually used, which adds the system complexity and cost. By incorporating individual DC/DC converter with independent controller for each PV module within the array, DMPPT technique aims at the PV-Module level partial shading or mismatch problem (Chen et al., 2014a) while differential power processing architecture aims at the submodule level mismatch (Jeon et al., 2017). However, since large number of DC/DC converters are required for the two techniques, the system cost and implementation complexity are increased. Furthermore, since either the full power or partial power will be processed by the DC/DC converters, the system efficiency is affected.

Without adding extra hardware components, many software based GMPPT strategies have been proposed (Bidram et al., 2012; Liu et al., 2015). Since tracking GMPP can be regarded as an optimization problem, many artificial intelligent (AI) methods have been proposed, such as particle swarm optimization (Ishaque et al., 2012; Ishaque and Salam, 2013; Sundareswaran et al., 2015a), fuzzy logic control (Alajmi et al., 2013; Boukenoui et al., 2016), genetic algorithm (Daraban et al., 2014), artificial neural network (Rizzo and

Scelba, 2015; Jiang et al., 2015), artificial bee colony (Sundareswaran et al., 2015b), firefly algorithm (Sundareswaran et al., 2014), grey wolf optimization (Mohanty et al., 2016), Ant-colony optimization(Sundareswaran et al., 2016), and simulated annealing (Lyden and Haque, 2016). These AI methods are effective for most shading patterns with high accuracy. However, the implementation of these AI methods is difficult since some parameters have to be carefully tuned and therefore the users must have certain professional knowledge on them (Bidram et al., 2012; Liu et al., 2015).

Another type of the GMPPT techniques are based on the mathematical expressions, such as Fibonacci technique (Ahmed and Miyatake, 2008) and dividing rectangle (DIRECT) technique (Nguyen and Low, 2010), which can regarded as segmental search method (Liu et al., 2015). With these techniques, the tracking range is firstly specified and gradually narrowed down until the final detection of the GMPP. Compared with the AI based strategies, the segmental search method is simpler and easier for the practical implementation. However, an appropriate initialization process is required in order to avoid the operating point trapped by the local MPPs (Bidram et al., 2012). Furthermore, if the segment division is inappropriate, this technique may overlook the GMPP (Liu et al., 2015).

Some researchers proposed new algorithms by modifying the conventional MPPT techniques to achieve the maximum power output under the PSCs (Patel and Agarwal, 2008; Chen et al., 2014b; Tey and Mekhilef, 2014; Wang et al., 2016). These GMPPT techniques generally assume all peaks, including LMPP and GMPP, approximatively locate at the multiple of $0.8V_{oc}$, which is referred as the $0.8V_{oc}$ model (Ahmed and Salam, 2015). However, their

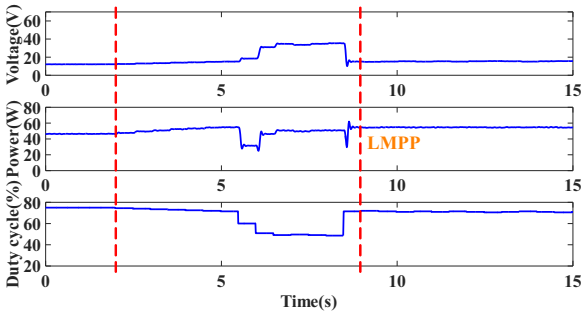

Fig. 3: Wrong tracking of the GMPPT techniques based on the $0.8V_{oc}$ model (Tey and Mekhilef, 2014).

tracking speed and tracking efficiency are affected considering that all peaks must be individually allocated with the P&O algorithm. Furthermore, these techniques may also overlook the exact GMPP (Liu et al., 2015). Fig. 3 shows the experimental results by using the GMPPT algorithm (Tey and Mekhilef, 2014). With this algorithm, a local MPP was tracked rather than the expected GMPP.

The power incremental method is proposed in (Koutroulis and Blaabjerg, 2012). The basic idea of this technique is that a large power interval is firstly employed for searching the whole P-V curve. Then, the operating point will be progressively moved towards a higher power level until further power increasing is not feasible. Compared to searching each vicinity of the $0.8V_{oc}$, the power incremental method only search the largest power, which is more direct. This technique is universal since it is effective for either grid-tied or standalone PV system and it can achieve the convergence to the GMPP under any PSC pattern. Furthermore, it is not necessary to know the internal connection or configuration within the PV array with this technique.

However, the power incremental method has two obvious disadvantages (Liu et al., 2015):

1. The performance of this technique is mainly determined by the search step. Specifically, a large step will result in the overlook of the GMPP while a small step may result in long tracking time.
2. It is difficult to directly use the power command to control the dc-dc converter. A special control circuit has to be used in this method.

Here, a novel power-increment based GMPPT algorithm is proposed. Compared to the conventional the $0.8V_{oc}$ model based GMPPT techniques, the proposed technique tracks the higher power level rather than the vicinity of $0.8V_{oc}$. Therefore, the proposed technique is faster than the $0.8V_{oc}$ model GMPPT techniques. Furthermore, the three lines, namely the power line, the voltage line and the load line, are used to determine the next moving position, which shows higher accuracy than the conventional power incremental method. Besides, the proposed technique provides a practical way to control the dc-dc converter, which does not need an additional control circuit. Finally, both simulation and experimental results under different partial shading conditions were presented to show the effectiveness of the proposed algorithm.

1. Proposed GMPPT technique

1.1. Duty cycle with the equivalent PV resistance

Fig. 4 shows the simplified connection of a PV system, where a dc-dc converter with MPPT control is used as an interface between a PV string

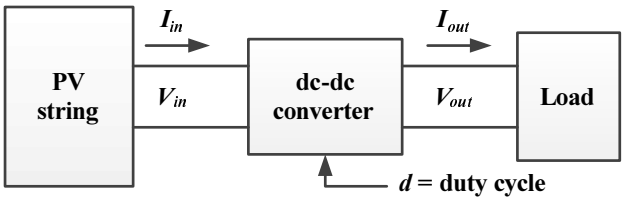

Fig. 4: Simplified connection of a PV system.

and a load. The control parameter d refers to the duty cycle of the converter. Assuming that $M(d)$ is the voltage conversion ratio, the mathematical expression for the input and output voltages of the dc-dc converter can be given by:

$$V_{in} = \frac{V_{out}}{M(d)} \tag{1}$$

$$I_{in} = M(d) \cdot I_{out} \tag{2}$$

Divide (1) by (2), it can be derived as:

$$R_{in} = \frac{V_{in}}{I_{in}} = \frac{V_{out}/M(d)}{M(d) \cdot I_{out}} = \frac{1}{M(d)^2} \cdot \frac{V_{out}}{I_{out}} = \frac{R_{out}}{M(d)^2} \tag{3}$$

where R_{in} and R_{out} represent the input and output resistance respectively. In a PV system, (3) can be rewritten as:

$$R_{pv} = \frac{R_{load}}{M(d)^2} \tag{4}$$

where R_{pv} refers to the equivalent resistance of the PV string, and R_{load} represents the load resistance.

Fig. 5 shows the basic principle of GMPPT for a PV string connected with a dc-dc converter. As illustrated in Fig. 5, a load line is used and imposed on the I-V curve of the PV string, where the slope of the load line θ can be written as:

$$\tan\theta = \frac{1}{R_{pv}} = \frac{M(d)^2}{R_{load}} \tag{5}$$

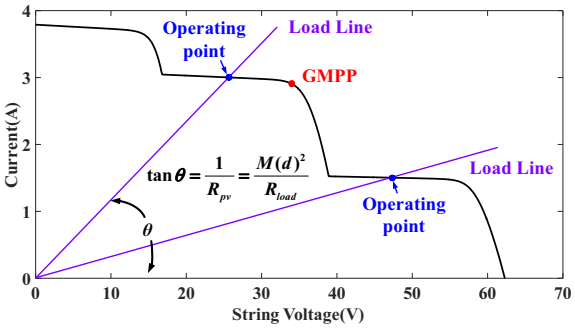

Fig. 5: Principle for GMPPT.

The operating point is determined by both the load line and the PV I-V curve. The duty cycle d can be controlled so that the operating point can be directed and moved along the I-V curve. At a certain value of d, the operating point will reach the GMPP to generate the maximum output power.

It should be noted that different dc-dc converters have different voltage conversion ratio $M(d)$, as summarized in Table 1. Taking buck-boost as an example, its $M(d)$ is shown as below:

$$M(d) = -\frac{d}{1-d} \tag{6}$$

Substitute (6) into (4), it can be derived as:

$$d = \frac{\sqrt{R_{load}}}{\sqrt{R_{load}} + \sqrt{R_{pv}}} \tag{7}$$

According to (7), if a desired R_{pv} is decided, the corresponding duty cycle d can be calculated, which guildes the movement of the operating point on the I-V curve.

Table 1: Summarization of voltage conversion ratio for different dc-dc converters

Converter	$M(d)$	d
Buck	d	$\frac{\sqrt{R_{load}}}{\sqrt{R_{pv}}}$
Boost	$\frac{1}{1-d}$	$1-\frac{\sqrt{R_{pv}}}{\sqrt{R_{load}}}$
Buck-Boost	$-\frac{d}{1-d}$	$\frac{\sqrt{R_{load}}}{\sqrt{R_{load}}+\sqrt{R_{pv}}}$
Cuk	$-\frac{d}{1-d}$	$\frac{\sqrt{R_{load}}}{\sqrt{R_{load}}+\sqrt{R_{pv}}}$
SEPIC	$\frac{d}{1-d}$	$\frac{\sqrt{R_{load}}}{\sqrt{R_{load}}+\sqrt{R_{pv}}}$

1.2. Flow chart of the proposed GMPPT

Based on (7), the modified power incremental method is proposed, as shown in Fig. 6.

Initially, the power incremental ΔP, the voltage incremental ΔV and the resistance load R_{load} should be initialized. These parameters are determined by the PV system, specifically, ΔP is tuned as $10W$, ΔV is tuned as $5V$, and R_{load} value is set as 20Ω. "Flag" is used to check whether the GMPP has been detected. Initially the value is 1 and once the GMPP is detected, "Flag" will be set as 0.

V_{min} is the low voltage boundary which should not be larger than the voltage value at the leftmost peak since the region in the left of V_{min} will not be searched. When the operating point works at the leftmost peak, the rest of PV modules in the PV string will be bypassed by anti-paralleled didoes.

Therefore, V_{min} can be approximately calculated by (Li et al., 2018)

$$V_{min} \leq 0.8 \cdot V_{oc} - (N-1)V_d \tag{8}$$

where N refers to the number of PV modules in a PV string, V_d refers to the voltage drop for bypass diodes. Taking V_{oc} as $21.1V$, V_d as $0.8V$ and the number of PV modules in the PV string is 3, (8) will be

$$V_{min} \leq 15.28 \tag{9}$$

Therefore, in this paper, V_{min} is set as $10V$.

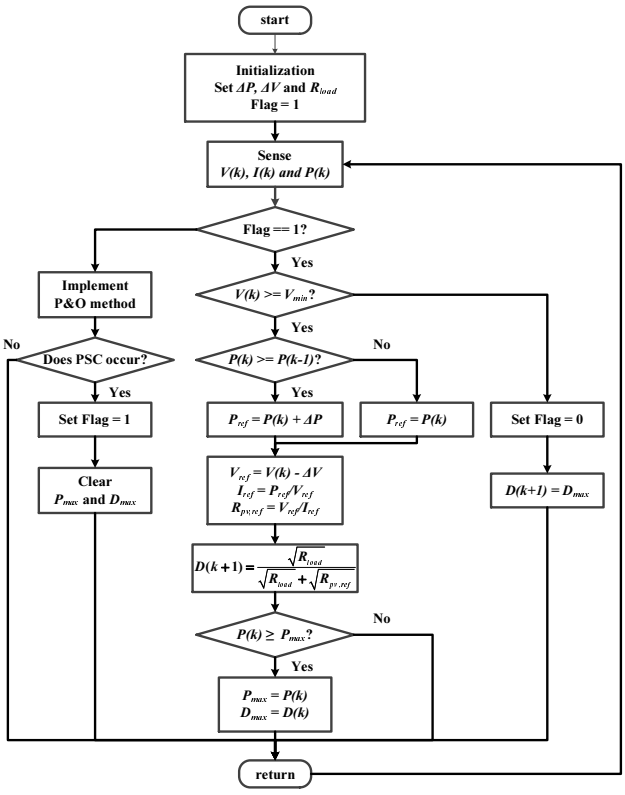

Fig. 6: Flowchart of the proposed technique.

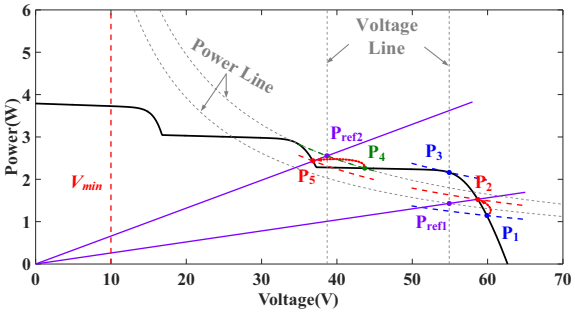

Fig. 7: Demonstration of the proposed technique.

1.3. Tracking process analysis

With the proposed algorithm, the tracking process with details is illustrated in Fig. 7. Assuming that the system starts at the operating point P_1. After the initialization, the present voltage $V(k)$ and current $I(k)$ will be measured and the present power $P(k)$ is calculated. Then, the reference power P_{ref} and voltage V_{ref} will be derived by:

$$P_{ref} = P(k) + \Delta P \tag{10}$$

$$V_{ref} = V(k) - \Delta V \tag{11}$$

After that, a power line and a voltage line will be imposed on the I-V curve by P_{ref} and V_{ref} respectively. The intersection of the power line and the voltage line will be the next desired point, P_{ref1}. However, this intersection may be not always on the I-V curve. Therefore, the load line $R_{pv,ref}$ is derived by

$$R_{pv,ref} = P_{ref}/V_{ref} \tag{12}$$

Then, the intersection between $R_{pv,ref}$ and the I-V curve will be the exactly desired point, P_2. In order to move to P_2, the next duty cycle $D(k+1)$ will

be updated by

$$D(k+1) = \frac{\sqrt{R_{load}}}{\sqrt{R_{load}} + \sqrt{R_{pv,ref}}} \tag{13}$$

If the calculated present power $P(k)$ is found larger than the previous one $P(k-1)$, the algorithm will continue the aforementioned process until the operating point reaches the point P_4, as shown in Fig. 7. When the point P_3 moves to the point P_4, the algorithm detects that the value of power at P_4 is smaller than that at P_3. It indicates that P_3 is located at one of the peaks and P_4 is located between the peak P_3 and another peak. In order to avoid to overlook the next peak, the P_{ref} will be calculated by

$$P_{ref} = P(k) \tag{14}$$

Then, $D(k+1)$ will be updated by (13)

After updated by $D(k+1)$, the proposed technique will check whether $P(k)$ is smaller than the recorded maximum power P_{max}. If it is true, P_{max} and the corresponding duty cycle D_{max} will be updated.

The aforementioned process will be repeated until the operating point reaches the low voltage boundary V_{min}, as shown in Fig. 7. If the sensed voltage is lower than V_{min}, "Flag" will be set as 0 since the proposed technique finds the GMPP. Then, the operating point will be regulated to the recorded maximum point by updating $D(k+1)$ as D_{max}. Finally, the P&O method will be triggered to maintain the operating point working on the GMPP.

It should be noted that, if the PSC happens again, "Flag" will be set as 1. Then, P_{max} and D_{max} will be cleared, and the proposed technique will be repeated the aforementioned process to relocate the GMPP. In order to effectively detect the PSC occurrence, an critical value of power change ΔP_{crit}

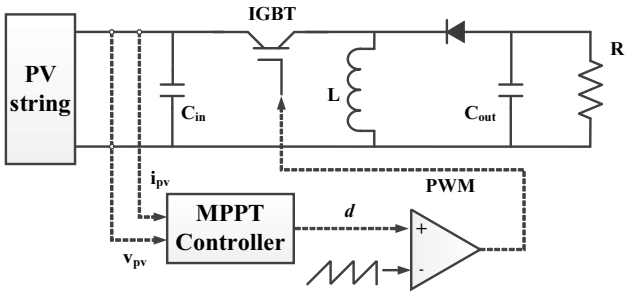

Fig. 8: System diagram of the PV system.

is generally used (Patel and Agarwal, 2008). In this paper, the condition "$\Delta P > \Delta P_{crit}$ is used to detect whether the PSC happens.

2. Simulation Evaluation

Fig.8 illustrates main system blocks of the PV system, including main components such as the PV string, power interface, load, and controller for the MPPT implementation are presented. A solar emulator is used with main electrical parameters listed in Table 2. The buck-boost converter is selected as the power interface and its main parameters include: the input capacitor C_{in} is $470uF$, the output capacitor C_{out} is $47uF$, the inductor for the buck-boost converter L is $1mH$, the switching frequency for the IGBT device is $20kHz$, and the resistive load is used with the value of 20Ω.

As illustrated in Fig.8, a direct MPPT control structure is used in this paper. Firstly, the controller senses the current i_{pv} and the voltage v_{pv} from the PV string, and generates duty cycle value d as an output. Then, the output d is sent to compared with a sawtooth signal, and finally generated the PWM to control the buck-boost converter. Since this direct MPPT control does not need any additional components, such as PI controller, the

Table 2: Key Parameters of the PV Module

Parameter	Symbol	Value
Maximum power	P_{mpp}	$60W$
Voltage at maximum power	V_{mpp}	$17.1V$
Current at maximum power	I_{mpp}	$3.5A$
Open-circuit voltage	V_{oc}	$21.1V$
Short-circuit current	I_{sc}	$3.8A$
Temperature coefficient of V_{oc}	K_v	$-80mV/^{\circ}C$
Temperature coefficient of I_{sc}	K_i	$0.065\%/^{\circ}C$

implementation of the MPPT techniques is relatively simple. Besides, T_p, which is the sampling time used in the the MPPT algorithm, is finally tuned as $0.03s$.

Fig.9 shows the three different PSC patterns. The first pattern is defined as the GMPP located in the rightmost peak while the second one is defined as the GMPP located in the middle peak. The location of the GMPP in the third pattern is set as the rightmost peak. However, it should be noted that the values of the other two peaks are very close to that of the GMPP, which is more challenged to the conventional power incremental method (Liu et al., 2015). Therefore, in this paper, these three PSC patterns will be used to evaluate the performance of the proposed algorithm.

Fig.10 shows main simulation results with the proposed algorithm for the first pattern of PSC. The details of the tracking process is given in Fig. 11 in order to clearly illustrate the tracking process.

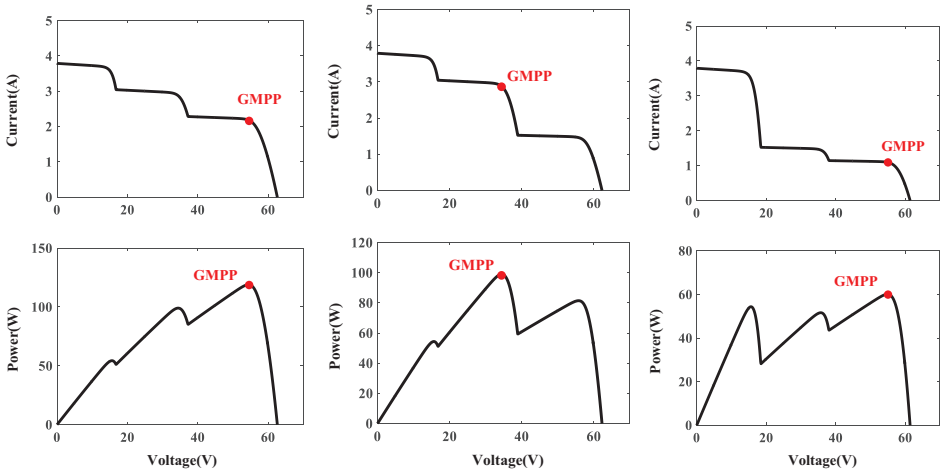

Fig. 9: Different PSC patterns.

At time $0s$, the system starts up, and operating point moves to the point P_1 at time $0.03s$. Then, the power line and the voltage are imposed on the I-V curve by (10) and (11), and the intersection point between these lines is the desired point, P_{ref}, marked as purple in Fig. 11(a). As shown in Fig. 11(a), P_{ref} is not on the I-V curve. Therefore, the load line, which is determined by (13), goes through P_{ref} to intersect with I-V, and the intersection point between the load line and I-V is the exact desired point P_2.

Then, the tracking process is repeated following the trajectory $P_1 \rightarrow \cdots \rightarrow P_6$. At time $0.18s$, P_{ref} is determined by (10) and (11), as shown in Fig. 11(b). Then, the exact desired point P_7 is determined by (13), marked as green in in Fig. 11(b).

Since the value of power at P_7 is smaller than P_6, in the next time, P_{ref} will be derived by:

$$P_{ref} = P(k) \tag{15}$$

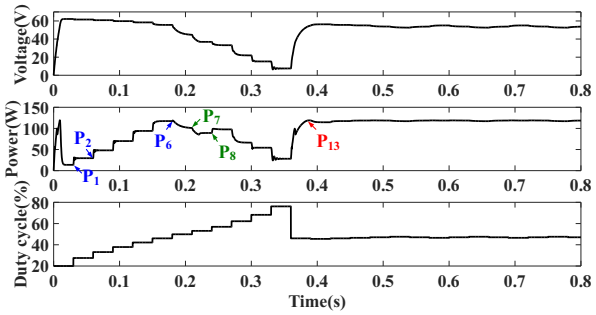

Fig. 10: Simulation results of the proposed technique for the first pattern.

namely the next P_{ref} will be at the same power line with P_7, as illustrated in Fig. 11(c). The reason for that is to avoid the overlook the next peak.

Then, the tracking process continues and follows the trajectory $P_8 \rightarrow \cdots \rightarrow P_{12}$. At time $0.36s$, P_{12} reaches the lower voltage boundary V_{min}. Thus, "Flag" is set as 0 since the proposed technique finds the GMPP. Then, the operating point will move to the recorded maximum point, namely P_{13} (P_6), by updating $D(k+1)$ as D_{max}. Finally, the P&O method is triggered to maintain the operating point working on the GMPP, marked as red in Fig. 11(d).

Fig.12 shows the simulation results of the proposed algorithm for the second PSC pattern. At time $0.15s$, the proposed technique finds the rightmost peak at P_5. Then, the middle peak, P_8, is found at time $0.24s$. At time $0.33s$, P_{11} reaches the lower voltage boundary V_{min}, and the operating point will move back to P_{12} (P_8), which is the recorded maximum point. Finally, the P&O method goes on, and the operating point working around P_{12}.

Fig.13 shows the simulation results of the proposed algorithm for the third PSC pattern. At time $0.12s$, the rightmost peak P_4 is found. Then,

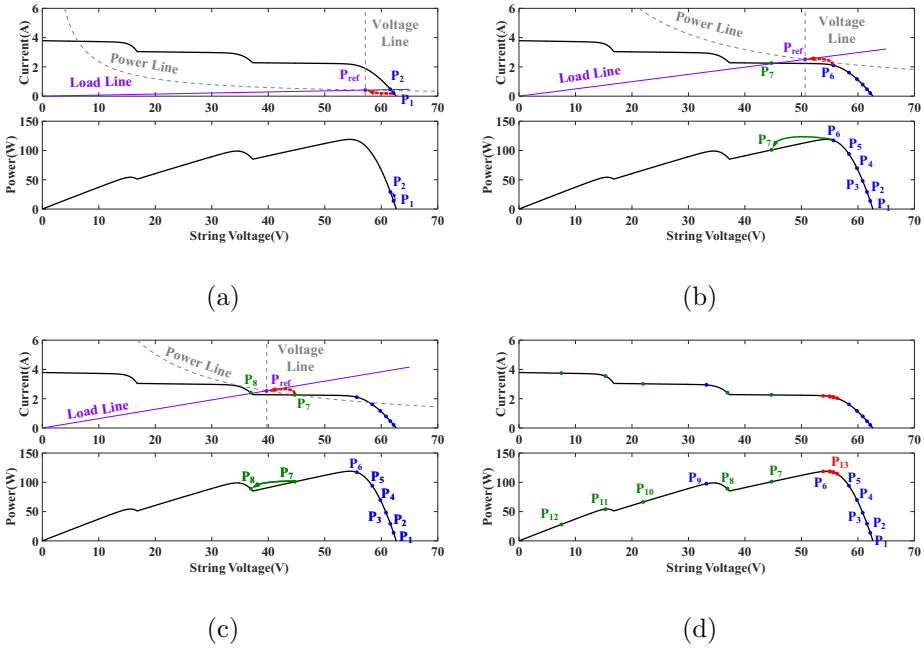

Fig. 11: Tracking process analysis for the first PSC pattern.

the next two peaks P_6 and P_9 are found at time $0.18s$ and $0.27s$ respectively. It should be noted that the values of P_4, P_6 and P_9 are very close, which is a great challenged to the conventional power incremental method. However, as illustrated in Fig.13, the proposed algorithm is able to located the GMPPT at P_4. Then, at time $0.3s$, P_{10} reaches the lower voltage boundary V_{min} and the operating point will move back to the recorded maximum point P_{11} (P_4). Finally, the P&O method will be executed and the exact location of the GMPP can be located and maintained.

3. Experiment

An experimental prototype was built, as shown in Fig.14, to validate the proposed algorithm. Table 3 shows main parameters for the key components

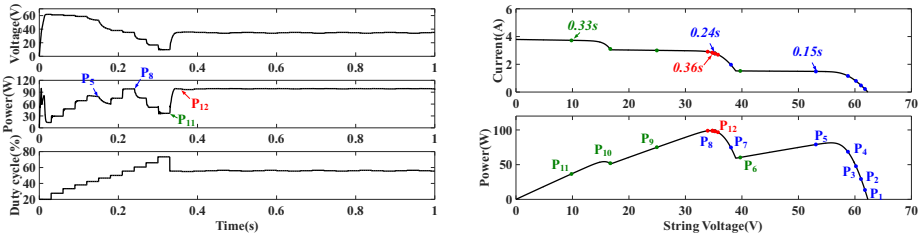

(a) (b)

Fig. 12: Simulation results of the proposed technique for the second PSC pattern.

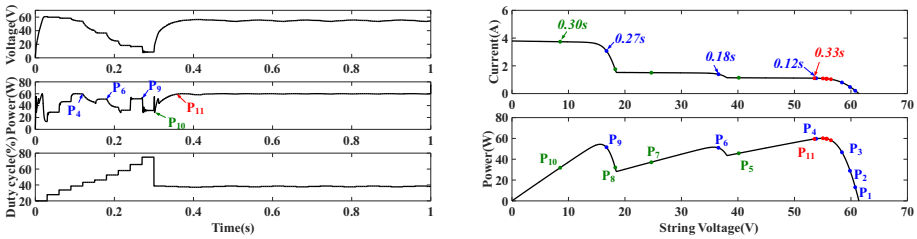

(a) (b)

Fig. 13: Simulation results of the proposed technique for the third PSC pattern.

of the converter.

Fig.14 shows the picture of the experimental prototype, which consists of a PV emulator, a dSPACE controller, a buck-boost converter and a load. Chroma ATE-62050H-600S is used as the PV emulator, where the user-defined I-V curves can be used to emulate solar module characteristics by its software panel. The dSPACE DS1104 implements the proposed technique. The sensed current and voltage goes to the dSPACE, and the dSPACE generates the PWM signal to control the buck-boost. Main experimental results were recorded and the performance of the proposed algorithm was analyzed. T_p , which is defined as the sampling time in the proposed MPPT algorithm in the experiments, is tuned as $0.5s$.

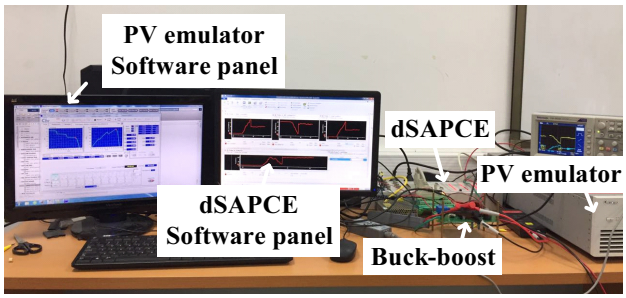

Fig. 14: Experimental prototype of the proposed PV system.

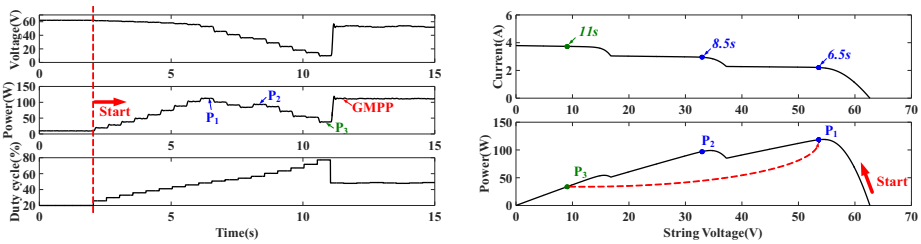

(a) (b)

Fig. 15: Experimental results of the proposed technique for the first pattern.

Same as the simulation setting, totally three PSC scenarios are used in experiments to evaluate the performance of the proposed algorithm. Fig.15 illustrates the experimental results for the first scenario. The period $0s$ to $2s$ is set as initial setting time, and the duty cycle is fixed at 20%. After $2s$, the proposed technique starts tracking. At time $6.5s$, the proposed technique finds the rightmost peak at P_1. Then, the middle peak, P_2, is found at time $8.5s$. At time $11s$, P_3 reaches the lower voltage boundary V_{min}. According to the recorded maximum power value, the GMPP is at the vicinity of P_1. Thus, the operating point will move back to P_1, and the P&O method goes on.

The experimental results for the second pattern is shown in Fig.16. The

Table 3: Main components for the buck-boost

Parameter	Value
Electrolytic capacitor C_{in}	$470uF$
Electrolytic capacitor C_{out}	$100uF$
Inductor L	$1mH$
IGBT	IRG4PH50U
Diode	RHRG30120
Current transducer	LA25-NP
Voltage transducer	LV25-P
Switching frequency	$20kHz$
Load	20Ω

proposed technique starts up tracking at time $2s$, and it only $2s$ to reach the first rightmost peak, P_1. Then, from P_1 to the next middle peak, P_2, the proposed technique uses $3.5s$. At time $10s$, the proposed technique reaches V_{min}, P_3, and moves back to the largest recorded power point P_2. Finally, the P&O method will be executed and finally the location of the GMPP can be located and maintained.

The experimental results for the third PSC pattern are illustrated in Fig.17. Similar to the first and second pattern, the period between $0s$ and $2s$ is initial setting time. The rightmost peak P_1 and middle peak P_2 are found at time $4s$ and $5.5s$ respectively. Then, at time $9s$, V_{min} is reached, and finally the operating point moves back to P_1 and the P&O method is triggered.

Fig.18 illustrates the experimental comparison among three different tech-

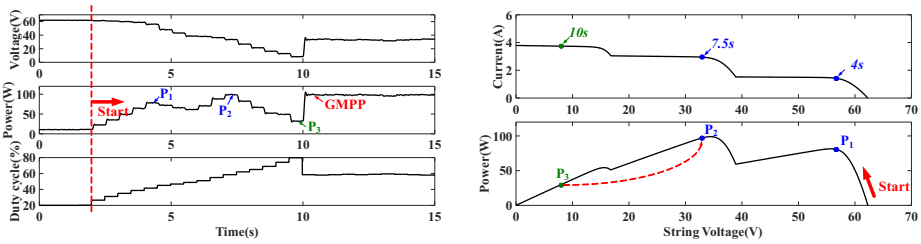

(a) (b)

Fig. 16: Experimental results of the proposed technique for the second pattern.

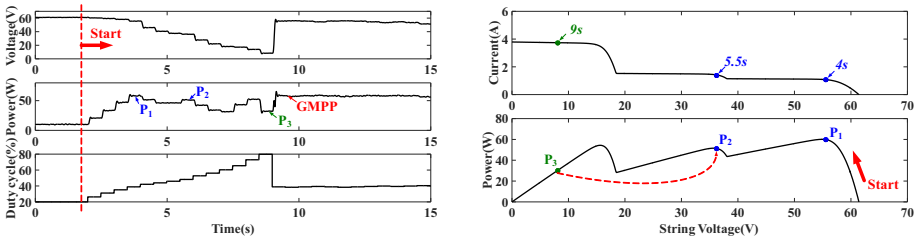

(a) (b)

Fig. 17: Experimental results of the proposed technique for the third pattern.

niques for the three PSC patterns. The proposed method is compared with the conventional power increment method (Koutroulis and Blaabjerg, 2012) and a typical $0.8V_{oc}$ model method (Tey and Mekhilef, 2014). In order to make a fair comparison, ΔP for the conventional power increment method is also set to $10W$. Furthermore, dynamic tracking efficiency is defined to evaluate the tracking performance for these three techniques:

$$\eta_{dyn} = \frac{\sum_0^{T_M} P_{pv}}{P_{max} \cdot T_M} \tag{16}$$

where P_{pv} represents the actual measured PV output power, P_{max} represents the theoretical maximum output power, and T_M is the measured tracking time. Besides, considering that a successful steady-state operation shows

three-level oscillations (Femia et al., 2005), here four cycle are considered in the steady-state efficiency calculation and the expression is given by:

$$\eta_{stat} = \frac{\sum_{T_M}^{T_M+4\cdot T_p} P_{pv}}{P_{max} \cdot 4 \cdot T_p} \tag{17}$$

Finally, Table 4 summarized main experimental results, where the term "Time" represents the tracking time for GMPP, "Tracking" and "Steady-state" are the dynamic and steady-state tracking efficiency respectively.

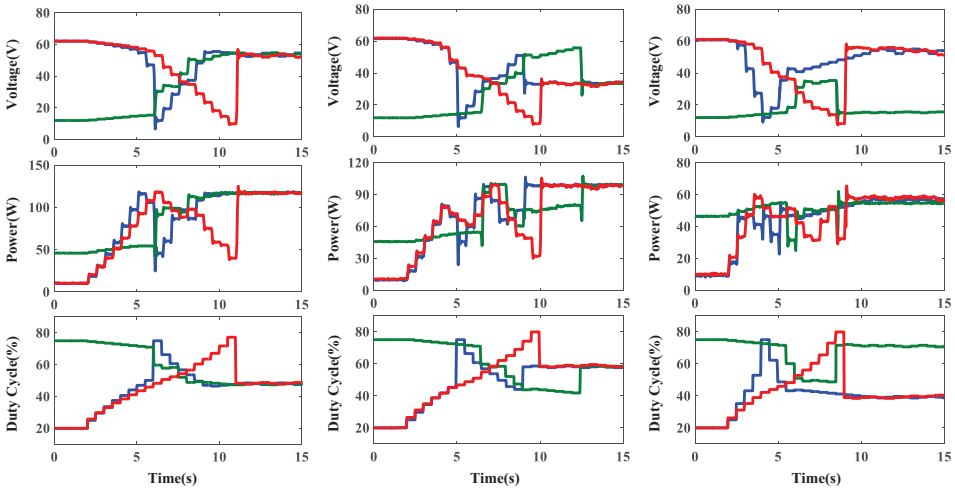

(a) (b) (c)

Fig. 18: Experimental comparison among Technique in (Koutroulis and Blaabjerg, 2012) (in blue), Technique in (Tey and Mekhilef, 2014) (in green) and the proposed method (in red). (a) First pattern; (b) Second pattern; (c) Third pattern.

Fig.18 (a) and (b) show the tracking performance for the first and the second pattern. It illustrates that the tracking speed of the proposed method is slightly slower than the conventional power increment method. However, the dynamic tracking efficiency of the proposed method and the conventional power increment method are very close. Furthermore, for the third pattern,

the proposed method requires less tracking time and higher dynamic tracking efficiency than the conventional power increment method. The reason for it is that the conventional power increment method is difficult to identify the GMPP for the third pattern. As shown in Fig.18 (c), the conventional power increment method has to use the P&O method to perturb ten steps in order to reach the GMPP, while the proposed method does not need it. Therefore, it proves that the proposed method shows more advantages compared with other two methods when the LMPP is very close to the GMPP. In addition, the method in (Tey and Mekhilef, 2014) shows slower tracking speed and lower dynamic tracking efficiency under the three patterns. It makes misjudgements and works at the LMPP for the third pattern. As a consequence, the steady-state tracking efficiency of the method discussed in (Tey and Mekhilef, 2014) is lower than the other two methods.

4. Conclusion

Considering the drawbacks of some GMPPT algorithms for PSC such as low tracking speed, overlook of GMPPs under some PSC patterns, and difficult-to-implement, a novel power incremental method is proposed here. The modulation of the duty cycle, rather than power commend, is used by the proposed technique to locate the desired point. Thus, compared to the conventional power incremental method, the difficulty to use the power command to control the dc-dc converter is overcame. Furthermore, the effectiveness of the proposed algorithm is verified under various PSCs with both the simulation and experimental results. Under the considered various PSC patterns, the tracking speed is fast and there is no overlook on each

Table 4: **Comparison of the experimental results for different PSC patterns**

Technique	First Pattern			Second Pattern			Third Pattern			
	Success	Time	Tracking	Success	Time	Tracking	Success	Time	Tracking	Steady-state
Technique in (Koutroulis and Blaabjerg, 2012)	Yes	8.0s	72.70%	Yes	7.0s	76.30%	Yes	8.0s	83.83%	98.05%
Technique in (Tey and Mekhilef, 2014)	Yes	8.5s	69.37%	Yes	11.0s	69.54%	No	6.5s	89.19%	90.18%
Proposed technique	Yes	9.0s	71.68%	Yes	8.0s	73.60%	Yes	7.0s	88.07%	98.05%

peak. As a conclusion, the proposed technique has an overall good tracking performance with fast tracking speed and accuracy.

5. Reference

Ahmed, J., Salam, Z., Dec. 2015. An improved method to predict the position of maximum power point during partial shading for pv arrays. IEEE Trans. Ind. Informat. 11 (6), 1378–1387.

Ahmed, N. A., Miyatake, M., 2008. A novel maximum power point tracking for photovoltaic applications under partially shaded insolation conditions. Electr. Pow. Syst. Res. 78 (5), 777–784.

Alajmi, B. N., Ahmed, K. H., Finney, S. J., Williams, B. W., Apr. 2013. A maximum power point tracking technique for partially shaded photovoltaic systems in microgrids. IEEE Trans. Ind. Electron 60 (4), 1596–1606.

Bidram, A., Davoudi, A., Balog, R. S., Oct. 2012. Control and circuit techniques to mitigate partial shading effects in photovoltaic arrays. IEEE J. Photovoltaics 2 (4), 532–546.

Boukenoui, R., Salhi, H., Bradai, R., Mellit, A., 2016. A new intelligent mppt method for stand-alone photovoltaic systems operating under fast transient variations of shading patterns. Sol. Energy 124, 124 – 142.

Chen, C. W., Chen, K. H., Chen, Y. M., Sept. 2014a. Modeling and controller design of an autonomous pv module for dmppt pv systems. IEEE Transactions on Power Electronics 29 (9), 4723–4732.

Chen, K., Tian, S., Cheng, Y., Bai, L., Jul. 2014b. An improved mppt controller for photovoltaic system under partial shading condition. IEEE Trans. Sustain. Energy 5 (3), 978–985.

Daraban, S., Petreus, D., Morel, C., 2014. A novel mppt (maximum power point tracking) algorithm based on a modified genetic algorithm specialized on tracking the global maximum power point in photovoltaic systems affected by partial shading. Energy 74, 374 – 388.

Drif, M., Perez, P. J., Aguilera, J., Aguilar, J. D., 2008. A new estimation method of irradiance on a partially shaded pv generator in grid-connected photovoltaic systems. Renewable Energy 33, 2048–2056.

Elgendy, M., Zahawi, B., Atkinson, D., Jan. 2013. Assessment of the incremental conductance maximum power point tracking algorithm. IEEE Trans. Sustain. Energy 4 (1), 108–117.

Elgendy, M., Zahawi, B., Atkinson, D., Mar. 2015. Operating characteristics of the p amp;o algorithm at high perturbation frequencies for standalone pv systems. IEEE Trans. Energy Convers. 30 (1), 189–198.

Femia, N., Petrone, G., Spagnuolo, G., Vitelli, M., Jul. 2005. Optimization of perturb and observe maximum power point tracking method. IEEE Trans. Power Electron. 20 (4), 963–973.

Hu, Y., Zhang, J., Li, P., Yu, D., Jiang, L., Sept. 2017. Non-uniform aged modules reconfiguration for large-scale pv array. IEEE Transactions on Device and Materials Reliability 17 (3), 560–569.

Ishaque, K., Salam, Z., Aug. 2013. A deterministic particle swarm optimization maximum power point tracker for photovoltaic system under partial shading condition. IEEE Trans. Ind. Electron 60 (8), 3195–3206.

Ishaque, K., Salam, Z., Amjad, M., Mekhilef, S., Aug. 2012. An improved particle swarm optimization (pso) based mppt for pv with reduced steady-state oscillation. IEEE Trans. Power Electron. 27 (8), 3627–3638.

Jeon, Y. T., Lee, H., Kim, K. A., Park, J. H., Mar. 2017. Least power point tracking method for photovoltaic differential power processing systems. IEEE Transactions on Power Electronics 32 (3), 1941–1951.

Jiang, L. L., Nayanasiri, D., Maskell, D. L., Vilathgamuwa, D., 2015. A hybrid maximum power point tracking for partially shaded photovoltaic systems in the tropics. Renew. Energy 76, 53 – 65.

Koutroulis, E., Blaabjerg, F., Apr. 2012. A new technique for tracking the global maximum power point of pv arrays operating under partial-shading conditions. IEEE J. Photovoltaics 2 (2), 184–190.

Li, X., Wen, H., Jiang, L., Hu, Y., Zhao, C., Sep. 2016a. An improved beta method with auto-scaling factor for photovoltaic system. IEEE Trans. Ind. Appl. 52 (5), 4281–4291.

Li, X., Wen, H., Jiang, L., Xiao, W., Du, Y., Zhao, C., Nov. 2016b. An improved mppt method for pv system with fast-converging speed and zero oscillation. IEEE Trans. Ind. Appl. 52 (6), 5051–5064.

Li, X., Wen, H., Y.Hu, Jiang, L., Xiao, W., Apr. 2018. Modified beta algorithm for gmppt and partial shading detection in photovoltaic systems. IEEE Power Electron. 33 (3), 2172–2186.

Liu, Y.-H., Chen, J.-H., Huang, J.-W., 2015. A review of maximum power point tracking techniques for use in partially shaded conditions. Renew. Sust. Energ. Rev. 41, 436–453.

Lyden, S., Haque, M. E., Jun. 2016. A simulated annealing global maximum power point tracking approach for pv modules under partial shading conditions. IEEE Trans. Power Electron. 31 (6), 4171–4181.

Mohanty, S., Subudhi, B., Ray, P. K., Jan. 2016. A new mppt design using grey wolf optimization technique for photovoltaic system under partial shading conditions. IEEE Trans. Sustain. Energy 7 (1), 181–188.

Nguyen, T. L., Low, K. S., Oct. 2010. A global maximum power point tracking scheme employing direct search algorithm for photovoltaic systems. IEEE Trans. Ind. Electron 57 (10), 3456–3467.

Patel, H., Agarwal, V., Apr. 2008. Maximum power point tracking scheme for pv systems operating under partially shaded conditions. IEEE Trans. Ind. Electron 55 (4), 1689–1698.

Petrone, G., Spagnuolo, G., Teodorescu, R., Veerachary, M., Vitelli, M., July 2008. Reliability issues in photovoltaic power processing systems. IEEE Transactions on Industrial Electronics 55 (7), 2569–2580.

Rizzo, S. A., Scelba, G., 2015. Ann based mppt method for rapidly variable shading conditions. Appl. Energy 145, 124 – 132.

Soon, T. K., Mekhilef, S., 2014. Modified incremental conductance mppt algorithm to mitigate inaccurate responses under fast-changing solar irradiation level. Sol. Energy 101 (0), 333 – 342.

Sundareswaran, K., kumar, V. V., Palani, S., 2015a. Application of a combined particle swarm optimization and perturb and observe method for mppt in pv systems under partial shading conditions. Renew. Energy 75, 308 – 317.

Sundareswaran, K., Peddapati, S., Palani, S., Jun. 2014. Mppt of pv systems under partial shaded conditions through a colony of flashing fireflies. IEEE Trans. Energy Convers. 29 (2), 463–472.

Sundareswaran, K., Sankar, P., Nayak, P. S. R., Simon, S. P., Palani, S., Jan. 2015b. Enhanced energy output from a pv system under partial shaded conditions through artificial bee colony. IEEE Trans. Sustain. Energy 6 (1), 198–209.

Sundareswaran, K., Vigneshkumar, V., Sankar, P., Simon, S. P., Nayak, P. S. R., Palani, S., Feb. 2016. Development of an improved p&o algorithm assisted through a colony of foraging ants for mppt in pv system. IEEE Trans. Ind. Informat. 12 (1), 187–200.

Tey, K. S., Mekhilef, S., Oct. 2014. Modified incremental conductance algorithm for photovoltaic system under partial shading conditions and load variation. IEEE Trans. Ind. Electron 61 (10), 5384–5392.

Wang, Y., Li, Y., Ruan, X., Jan. 2016. High-accuracy and fast-speed mppt

methods for pv string under partially shaded conditions. IEEE Trans. Ind. Electron 63 (1), 235–245.